Indian J. Phys. **81(11)** 1177-1204 (2007)

Review

IJP

Diffusion and mobility driven instabilities in a reaction-diffusion system : a review

Syed Shahed Riaz and Deb Shankar Ray*

Department of Physical Chemistry, Indian Association for the Cultivation of Science, Jadavpur, Kolkata 700 032, India

E-mail : pcdsr@mahendra.iacs.in

Abstract : Interplay of reaction and diffusion in a chemical system may lead to many interesting selforganization phenomena like stationary pattern, waves, spirals and targets *etc.* in spatially extended nonlinear dynamical systems far from equilibrium. One may trace their origin to different instabilities. In this review we have presented a pedagogical exposition of two such instabilities relating to stationary pattern formation. The first one is the diffusion-driven instability, the Turing instability, arising from disparate diffusivities of two reacting components in a reaction-diffusion system under appropriate condition. The second one is the differential flow induced chemical instability which can be brought in by application of electric and magnetic fields. The analysis of instabilities and simulation of patterns have been carried out on chlorine dioxide-iodine-malonic acid reaction (CDIMA), which has served as an experimental testing ground for various theories in the last two decades.

Keywords : Reaction diffusion system; pattern formation Hopf bifurcation, Turning instability

PACS Nos : 82.40. Ck 7.54. +r 05.45. -a

Plan of the Article

* Corresponding Author

1. Introduction

Evolution of order or pattern is a phenomenon ubiquitous to almost every branch of science, starting from physical systems to chemistry or biology. The question that how systems realize such high degree of ordering, from very simple basic principles has allured the scientific world for ages. Ordering can be seen in both time and space domains. The examples of temporal order, that is oscillations are quite common. In chemistry there is a class of reactions which are oscillatory in nature. The first ever reported chemical oscillation was due to Fechner in 1828 [1] who described an electrochemical cell producing oscillatory current. Ostwald observed in 1899 [4] that the rate of chromium dissolution in acid varies periodically in time. However since both the examples come from inhomogeneous systems the impression then was that homogeneous oscillation was impossible. It was W. C. Bray who provided the first counterexample [2,3]. He noted in the reaction between iodate, iodine and hydrogen peroxide, the rate of evolution of oxygen and the iodine concentration changes periodically. However during the next fifty years the chemistry community would reject the claim about the homogeneity of the reaction and engage themselves in believing that the oscillation was an artifact of dust and bubbles. The final breakthrough in this field was brought about, however, by a Russian chemist, Boris Pavlovich Belousov who, looking for some inorganic analogue of Krebs cycle was investigating a solution of bromate, citric acid and ceric ions. He noted the periodic conversion of yellow Ce(III) and colourless Ce (IV) [5,6]. His finding was however outwardly rejected by the established journals. This is mainly because the scientific community in those days was suffering from the prejudice that the occurrence of chemical oscillation tends to violate the second law. But there was no such violation was obvious if one realizes that in these oscillatory reactions only the intermediates oscillate in time and not the reactants or products. So to get sustained oscillations one has to supply the reactants steadily by keeping the system open.

One more oscillatory process which has gained importance recently due to the reason we will elaborate later is the chlorine-di-oxide-iodine-malonic acid system (CDIMA) [7–10,14,15]. Such oscillations are however most common in biology. There the stable oscillations are a must in order to keep the living body working. Some extensively studied biological oscillatory processes are the glycolytic cycle, circadian rhythm, Ca^{+2}-oscillation or the cell cycle.

When diffusion is introduced into the reaction kinetics, nonlinear dynamics of the system becomes significantly richer. One encounters stationary, spatially-varying concentration or patterns, traveling waves, spiral and targets. To realize spatial structure one must consider, of course, spatially extended systems where the dynamics at various spatial points gets coupled through diffusion. Such a reaction-diffusion model that explains the generation of spatial patterns was first put forward by Alan Turing in 1952 [16]. He worked out a theory of morphogenesis to show that a coupling between the reaction among two species of different diffusivities and the diffusion process may result in stationary concentration patterns observed in the biological world. The patterns in the skin of tiger, leopard, zebra or in butterfly wings are few most enthralling examples. Such spatial structures are not limited solely within the premises of

biological sciences. However, because of a stringent necessary condition that diffusion of one of the components must be much faster compared to that of the other and the lack of realization of an open thermodynamic system, experimental observation of Turing pattern remained elusive for nearly four decades after its theoretical prediction. With the development of suitable chemical systems where kinetics includes a positive feedback and widely different effective diffusivities of the two reacting species, unambiguous experimental evidences on Turing pattern were clearly established in the last decade of 20th century. Since then theoretical and experimental studies gathered a new momentum. An important endeavor in this development is how the oscillation, wave propagation and patterns are affected by external fields. It has been demonstrated that applying fields can have a profound effect on the propagation of waves in ionic chemical reactions, *e.g.*, by causing wave splitting, annihilation, acceleration and production of spiral from targets *etc.* A constant electric field may also generate a differential flow induced stationary patterns or destabilize it under appropriate condition. The possibility of using electric field as a control parameter for reaction front instabilities has also been examined.

Our object in this review is to explore two types of instabilities centering around these developments. First, we outline the basic pedagogical background that leads to stationary Turing pattern followed by a discussion on the related experimental aspects . Second, while Turing instability concerns disparate diffusivities we extend the theoretical scheme further to analyze the role of different mobilities in controlling differential flow leading to instabilities and pattern formation. The testing ground for theoretical and numerical analysis of these instabilities is the prototype reaction diffusion system, CDIMA reaction.

2. Diffusion-driven instability : theoretical and experimental aspects

A. Turing pattern :

Turing's idea was elegant but surprisingly simple [16]. Before proceeding further we need to consider his viewpoint in some detail.

We consider two reactants *A* and *B*. In absence of diffusion they react to reach some steady state. Now this steady state can be stable or not. Turing raised the question whether diffusion can bring in instability to an otherwise homogeneous stable steady state. Analysis revealed that this is possible provided the rates of diffusion of the two species widely differ. The idea is novel as it contradicts the wellknown stabilizing role of diffusion. Before going through the analytical details it would be useful to grasp the pith of the theory intuitively.

Consider an auto-catalytic reaction mechanism which involves an 'activator' that diffuses slowly compared to 'inhibitor'. Let by shear chance a small region of space sees a sudden rise in activator concentration. This in turn enhances the reaction rate and as a consequence concentration of both the species grow. Now the inhibitor diffuses out at a faster rate compared to the activator. The result is that a small region in space becomes richer in activator surrounded by an area richer in inhibitor. Thus any small perturbation of concentration grows in time and an inhomogeneity results.

We now present the analysis of Turing in a somewhat modified form. If we consider a model of two chemical species in one dimension where one is acting like an activator $u(x, t)$ and other as an inhibitor $v(x, t)$ then the corresponding reaction-diffusion equations are given by

$$\begin{aligned} u_t &= \gamma f(u,v) + \nabla^2 u \\ v_t &= \gamma g(u,v) + d\nabla^2 v \end{aligned} \tag{1}$$

where $d = D_v / D_u$, is the ratio of the diffusion coefficients of the species v and u, respectively and γ is the constant related to the length scale of the problem. The parameter space has to be chosen in such a way that in absence of diffusion both u and v tend to linearly stable steady state which is homogeneous in nature. In presence of diffusion where $D_v \neq D_u$ the spatially stationary inhomogeneous patterns may develop under certain conditions by diffusion-driven instability. The uniqueness of this concept lies in the fact that diffusion which is usually considered as a stabilizing process is responsible for causing the instability.

We begin by looking for the necessary and sufficient conditions for diffusion-driven instability of the homogeneous steady state and the initiation of spatial pattern for such a general system given by eq.(1). Following Turing we impose the zero flux boundary conditions. The relevant homogeneous steady state (u_0, v_0) of eq.(1) is given by

$$f(u_0, v_0) = 0, \qquad g(u_0, v_0) = 0. \tag{2}$$

Now in absence of diffusion u and v satisfy

$$u_t = \gamma f(u,v), \qquad v_t = \gamma g(u,v). \tag{3}$$

Linearizing around the steady state (u_0, v_0) *i.e.* assuming $u = u_0 + \delta u$ and $v = v_0 + \delta v$, we ultimately arrive at the dynamical equations for the perturbations δu and δv as,

$$y_t = \gamma A y, \qquad A = \begin{pmatrix} f_u & f_v \\ g_u & g_u \end{pmatrix} \tag{4}$$

where A is known as the stability matrix comprising of partial derivatives of f and g with respect of u and v, respectively, evaluated at the steady state (u_0, v_0). In eq. (4) y is defined as

$$y = \begin{pmatrix} \delta u \\ \delta v \end{pmatrix}. \tag{5}$$

We now look for solutions of the form

$$y \sim e^{\lambda t} \tag{6}$$

where λ is the eigenvalue. For the steady to be linearly stable the real part of the eigenvalue should be less than zero which assures that the perturbation $y \to 0$ as $t \to \infty$. Proceeding as usual we are led to the following algebraic equation for the eigenvalues

$$\lambda^2 - \gamma(f_u + g_v)\lambda + \gamma^2(f_u g_v - f_v g_u) = 0. \tag{7}$$

From the above equation it is quite evident that the linear stability of the steady state is guaranteed if

$$f_u + g_u < 0, \qquad f_u g_u - f_v g_u > 0. \tag{8}$$

Since the steady state of a system is determined by the kinetic parameters the inequalities eq.(8) define the stability regions for the homogeneous steady state.

We now return to the full reaction-diffusion system eq.(6) and linearize it about the steady state to obtain

$$y_t = \gamma A y + D\nabla^2 y, \qquad D = \begin{matrix} 1 & 0 \\ 0 & d \end{matrix}. \tag{9}$$

Here, we allow (for simplicity, consider one dimension) the small perturbations in u and v *i.e.* δu and δv to grow spatially as well temporarily around (u_0, v_0) as $\delta u \sim e^{\lambda t}\cos kx$ and $\delta v \sim e^{\lambda t}\cos kx$, where k is the wavenumber. Application of zero flux boundary condition then results in $k = n\pi / a$. n is an integer and a determines the domain size in one dimension. Putting the aforesaid form of the perturbations in eq.(40) we ultimately arrive at an equation

$$\lambda^2 + \left[k^2(1+d) - \gamma(f_u + g_v)\right]\lambda + h(k^2) = 0 \tag{10}$$

where $h(k^2) = dk^4 - \gamma(df_u + g_v)k^2 + \gamma^2|A|$. $|A|$ is the determinant of the stability matrix A. From eq.(10) one comes out with a necessary condition for instability in presence of diffusion, $Re\lambda > 0$ as

$$df_u + g_v > 0. \tag{11}$$

The above equation demands that $d \neq 1$ and f_u and g_u must have opposite sign. Eq.(11) is necessary but not the sufficient condition for $Re\lambda > 0$ since it requires that $h(k^2)$ must be negative for some non-zero k *i.e.* the minimum h_{min} must be negative. The condition for which $h(k^2) < 0$ for some $k^2 \neq 0$ is

$$(df_u + g_v)^2 - 4d(f_u g_u - f_u g_u) > 0 \ . \tag{12}$$

This condition also highlights the fact that for a fixed set of kinetic parameter parameter values there is critical diffusion coefficient ratio d_c which must be greater than unity for initiation of spatial pattern formation. Again if we plot the dispersion relation *i.e.* the relation between λ and k^2 from eq. (10) when $d > d_c$, we find a range of wave-numbers $k_1^2 < k^2 < k_2^2$ for which the solution is linearly unstable Figure 1. With the zero flux boundary condition applied on the two dimensional domain $\left[x \in (0, L_x)\right.$ and $\left.y \in (0, L_y)\right]$, L_x and L_y being the domain size in x and y directions], we find that k^2 forms a discrete set of wave numbers such that $k^2 = k_x^2 + k_y^2$ and

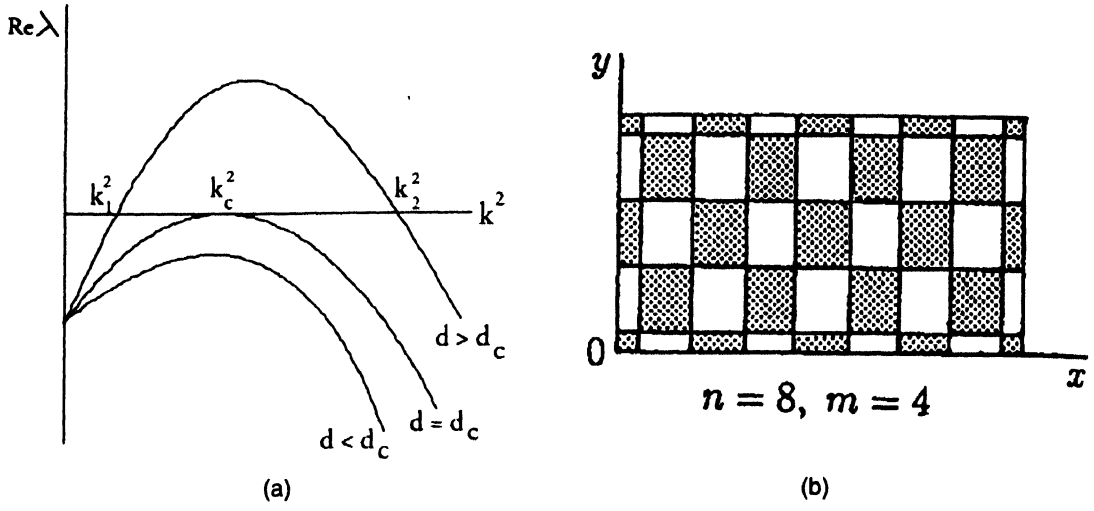

Figure 1. (a) Plot of the largest of the eigenvalues $\lambda(k^2)$ as a function of k^2. (b) Typical two-dimensional spatial patterns indicated by the linearly solution when various wavenumbers are in the unstable range. The shaded regions are where $u > u_0$, the uniform steady state.

$$k_x^2 = \frac{n^2\pi^2}{L_x^2},\ k_y^2 = \frac{m^2\pi^2}{L_y^2}\ (n, m \text{ being integers}).$$

Thus, the dispersion relation is extremely important and this determines the nature of eigen solutions which are linearly unstable and grow exponentially with time. It is also important to note that since we are dealing here with a finite domain eigenvalue problem, the wave-numbers are discrete because of boundary and so only a set of k values $\left| k_{n,m}^2 = \frac{n^2\pi^2}{L_x^2} \quad \frac{m^2\pi^2}{L_y^2} \right.$ shown in the Figure 1(a) (between k_1^2 and k_2^2) are relevant in this case. Figure1(b) shows the pattern of solution in this range. The nonlinearity of the kinetic terms however are there to restrict the linearly unstable solutions growing exponentially with time within a bounded region and to produce an ultimate steady spatially inhomogeneous pattern. It is also possible to extend the treatment for three dimensional reaction-diffusion systems and depending on the nature of nonlinearity one may observe set by eqs. 8,11,12.

Turning pattern has been the subject of wide attention in almost all major areas of natural sciences. Although the subject of pattern formation had been developed in early 1950's, it flourished in early 1990's after it's first unambiguous experimental verification in a classical system. Its experimental realization was hard primarily because the diffusion coefficients of most of the chemical species are very close to each other. In the next subsection we discuss how this difficulty was overcome.

B. CDIMA system : The experimental demonstration of Turning pattern :

The development of CDIMA system (CDIMA) system (Chlorine Dioxide-Iodine-Malonic acid) not only pioneered the experimental study in this field but also inspired extensive analytical and numerical studies that provided insight into the subject. The chemical reactions that are involved in the model are the following.

$$MA + I_2 \rightarrow IMA + I^- + H^+$$

$$ClOL_2 + I^- \rightarrow ClO_2^- + \frac{1}{2} I_2$$

$$ClO_2^- + 4I^- + 4H^+ \rightarrow Cl^{-+} + 2I_2 + 2H_2O$$

It is therefore, a five variable model if we identify the concentration of each of the reacting species as our variable. However in the course of reaction the concentrations of all the species but I^- and ClO_2^- remain more or less constant. This effectively reduces the model into a two variable one with concentrations of ClO_2^- and I^- being the relevant two variables. We now let $[I^-] \equiv X$ and $[ClO_2^-] \equiv Y$ and treating concentrations of all other species as constants we can simplify the above equations to reflect the behavior of the two variable species X and Y.

$$\rightarrow X$$

$$X \rightarrow Y$$

$$4X + Y \rightarrow$$

and the corresponding rates as

$$r_1 = k_1'$$

$$r_2 = k_2'[X]$$

$$r_3 = k_3' \frac{[X][Y]}{(\alpha + [X]^2)}$$

where $k_1' = k_{1a}[MA]$, $k_2' = k_2[ClO_2]$, $k_3' = k_{3b}[I_2]$, k_{1a}, k_2, k_{3b} are the rate constants of the three reactions, respectively.

Here, we have neglected the first term in the rate law. The resulting differential equations for [X] and [Y] are

$$\frac{\partial [X]}{\partial t} = k_1' - k_2'[X] - 4\frac{k_3'[X][Y]}{(\alpha + [X]^2)} \tag{13}$$

$$\frac{\partial [Y]}{\partial t} = k_2'[X] - \frac{k_3'[X][Y]}{(\alpha + [X]^2)}. \tag{14}$$

To make things simpler we define dimensionless variables $u = \frac{[X]}{\alpha^{\frac{1}{2}}}$, $v = \frac{k_3'[Y]}{k_2'\alpha}$, $\tau = k_2't$ and parameters $a = \frac{k_1'}{k_3'\alpha^{1/2}}$, $b = \frac{k_2'}{k_3'\alpha^{1/2}}$. Eq. (13) and (14) then can be written in the form

$$\frac{\partial u}{\partial \tau} = a - u - 4\frac{uv}{1+u^2} \tag{15}$$

$$\frac{\partial v}{\partial \tau} = b\left(u - \frac{uv}{1+u^2}\right) \tag{16}$$

The steady state of the system is given by $u_{ss} = \frac{a}{5}$, $v_{ss} = 1 + \frac{a^2}{25}$. The condition for stability of the system can be obtained applying eq. (8) and they are

$$b > \frac{3a}{a} + \frac{25}{a} \tag{17}$$

and

$$1 + (a/5)^2 - \frac{ab}{1+(a/5)^2} > 0. \tag{18}$$

Since condition (18) is satisfied by any a, b (remembering that they are always positive), condition (17) solely governs the stability of the state. This inequality defines a surface in the $[ClO_2]-[I_2]-[MA]$ plane that separates the regions of stable oscillation and steady state. Now to realize the possibility of pattern formation we have to consider spatially extended systems where the different spatial points are coupled through diffusion. We consider diffusion in two dimensions keeping in mind the experimental slab like reactor where the height of the slab is too small to allow any appreciable diffusion in that direction.

The dynamics is then given by

$$\frac{\partial u}{\partial \tau} = a - u - 4\frac{uv}{1+u^2} + D_u\nabla_u^2 \tag{19}$$

$$\frac{\partial v}{\partial \tau} = b\left[u - 4\frac{uv}{1+u^2}\right] + D_u\nabla_u^2. \tag{20}$$

Now let us suppose one of the reacting species *viz.* the iodide, complexes with some complexing agent (which might be starch). The motivation behind such a selective complexation will be revealed later. The complexation equilibria is represented as

$$S + u \rightleftharpoons S_u.$$

Now we modify eq. (19) to take into account the complexation and write down a rate equation for S_u

$$\frac{\partial v}{\partial \tau} = f(u,v) + D_u \nabla^2 u + k_b s_u - ku \tag{21}$$

$$\frac{\partial S_u}{\partial \tau} - -k_b S_u + ku \tag{22}$$

where $k = k_f S$ and $k' = \frac{k}{k_b} = k_s, k_f$ and k_b are the forward and reverse rate constants, respectively, of the complexation reaction.

Now assuming that the formation and dissociation of the complex are rapid, we replaced u by $k'S_u$. Such a substitution has been justified elsewhere [11].

We now add eq. (21) and eq. (22) and eliminate the concentration of the complex to obtain

$$\frac{\partial(u + Su)}{\partial t} = (1 + k')\frac{\partial u}{\partial t} - f(u,v) + D_u \Delta_u^2. \tag{23}$$

The final form of the reaction-diffusion equation is now

$$\frac{\partial u}{\partial t'} = f(u,v) + \nabla \tag{24}$$

$$\frac{\partial v}{\partial t'} = \sigma\left[g(u,v) + d\nabla_v^2\right] \tag{25}$$

where $\sigma = 1 + k', d = D_v / D_u, \quad t' = \sigma\tau$. Thus the complexation separates the time scales for the evolution of the activator and inhibitor by a factor σ. This exerts a stabilizing influence upon the steady state not affecting however, the steady state composition. The condition 17 now reads as

$$\sigma b > \frac{3a}{5} - \frac{25}{a}. \tag{26}$$

By the Poincare-Bendixon theorem, the system will have a periodic limit cycle whenever eq.(17) is violated. The Hopf curve given by $\sigma b = \frac{3a}{5} - \frac{25}{a}$ separates a, b phase into two regions. Above the curve the steady state is stable, below it gives away to homogeneous oscillation. With increasing σ the curve takes downward shift. To investigate the possibility of pattern formation we have to enquire under what condition a stable kinetic state gets unstable due to diffusion. The criteria for diffusion induced instability can be had from condition 12. For the present system the condition reads as

$$\left(3da^2 - 5ab - 125d\right)^2 \geq 100abd\left(25 + a^2\right) \tag{27}$$

The plot of *a vs b* according to eq. (27) gives the Turing line. Below this Turing curve the state loses its stability due to diffusion. So the Turing condition is held in a parameter zone above the Hopf and below the Turing curve. As obvious from Figure 2 such a situation may only be realized pattern.

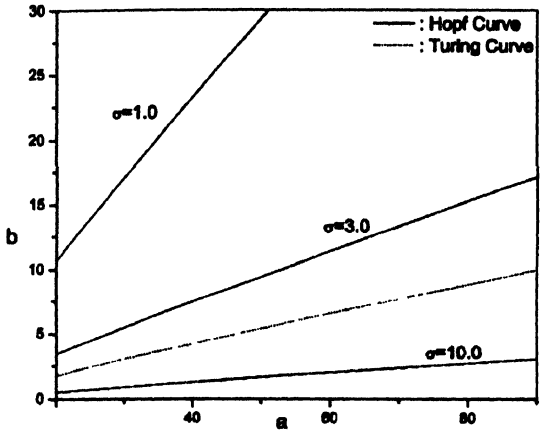

Figure 2. Bifurcation curve.

The first demonstration of Turing pattern was made with this CDIMA system [8]. At this juncture of our discussion one should recall what were the obstacles that were delaying the experimental realization of Turing pattern and in what way they are overcome due to the development of CDIMA system.

Firstly it follows from our earlier discussion that to get sustained Turing pattern, one needs an open system. By maintaining constant flow of some key species their concentrations should be kept constant. Moreover by perfect mixing the concentrations of these species have to be kept uniform in space as well. It is possible, however, to observe transient patterns in a closed system like Petri dish *e.g.* in BZ reaction. Also chemical oscillation in essentially homogeneous open system has also been done by introducing stirred flow reactors. By the late eighties a number of ideas were developed [18] in order to create open systems, among which the most notable is the use of gel as the reaction medium. In this method two broad faces of a slab of gel, composed, for example, of polyacrylamide or agar, are in contact with two solutions of different compositions. The solutions, which are circulated through CSTRs (continuous stirred tank reactor), contain the reactants for the reaction that give rise to the pattern formation. These reactants diffuse into the gel, encountering each other at significant concentrations in a region near the middle of the gel, where the pattern formation can occur. The CSTRs provide a continuous flow of fresh reactants, which diffuse into the gel, thereby maintaining the system as open. Next comes the difficulty with the constraint of differing diffusivity. This was very elegantly overcome by the use of gel as reactor. Here the added starch complexes with iodide and thereby reduces its mobility through the porous polyacrylamide gel compared to free chlorite. The mechanism was however realized a bit later [11].

3. Effect of electric field in generating instability due to differential flow

In the early nineties a new kind of instability was predicted for a system involving activator and inhibitor in a reactive flow. It was shown that differential flow of activator and inhibitor can

induce instability to a spatially homogeneous stable state just as differential diffusivity does in case of Turing instability. Such a condition of differential flow may be achieved by manipulating external conditions, *e.g.*, by applying fields, if however, the mobilities of the species due to field are different [12,13]. The instability here is therefore free from restriction on diffusivity of species and therefore is expected to occur in a wide variety of natural as well as artificial systems. In the present section we show that a symmetry breaking instability leading to formation of spatial structures may result in when a constant external electric field normal to the reaction plane causes a diffusion-driven stable state (in absence of diffusion the steady state is homogeneous and unstable due to Hopf bifurcation) to become unstable.

A. The reaction-diffusion system under external electric field :

Let us consider the simplest possible class of systems with two concentration variables $u(x, y, z, t)$ and $v(x, y, z, t)$ for activator and inhibitor, respectively, in three dimensions (x, y, z). The two species are, in general ionic in nature so that in presence of a constant electric field E along z direction, the space time evolution of the variables u and v are given by the following reaction-diffusion equations [65,66].

$$u_t = f(u,v) + z_1 E u_z + u_{xx} + u_{yy} + u_{zz} \tag{28}$$

$$v_t = g(u,v) + z_2 E d v_z + d v_{xx} + d v_{yy} + d v_{zz}\,. \tag{29}$$

Here $f(u, v)$, $g(u, v)$ are the functions representing the reaction terms, which allow a spatially uniform steady state u_0, v_0 such that $f(u_0, v_0) = g(u_0, v_0) = 0$. z_1, z_2 are the electric charges associated with activator and inhibitor, respectively, d is the ratio of their diffusion coefficients, which in view of Einstein relation is the same as the ratio of their respective mobilities. It is important to point out that formation of spatial inhomogeneity in internal electric field intensity and charge density due to interaction of diffusion and chemical reaction in ionic species, *e.g.*, in Brusselator model had been investigated earlier by Marek *et al* [67] in which the internal electric field is represented by the gradient of an electric potential. Electric field effects on propagation of chemical waves have attracted attention both from experimental and theoretical point of view [68,69]. We assume, however, that the electric field as employed here is external and small and neglect the effects of aforesaid inhomogeneities and ohmic heating and products of electrolysis (gas bubbles, for instance). Because of the occurrence of the first derivative terms along Z-direction it is not easy to carry out any straight forward linear stability analysis of the three dimensional system eqs. (28) and (29) that includes the effect of electric field and which is consistent with zero flux boundary conditions on all three directions. Since because of using thin gel as a reactor in experiments, the quasi-two-dimensional stationary spatial structures are of major interest. Following Lengyel *et al* [63] it is therefore convenient to approximate the real three-dimensional system to a quasi-two-dimensional system for stability analysis by replacing the forcing term along z-direction with its discrete representation considering a thin layer with thickness L. The gradients in the following terms in z-direction can be approximated by are the averages of the respective steady state concentrations just above

and below the layer concerned. Eqs. (28) and (29) can therefore be modified as $u_z = (u - \bar{u}_0)/L$; $v_z = (v - \bar{v}_0)/L$; $u_{zz} = 2(u - \bar{u}_0)/L^2$; $v_{zz} = 2(v - \bar{v}_0)/L^2$; where $\bar{u}_0$ and $\bar{v}_0$ are the averages of the respective steady state concentrations just above and below the layer concerned. Eqs. (28) and (29) can therefore be modified as

$$u_t = F(u,v) + u_{xx} + u_{yy} \tag{30}$$

$$v_t = G(u,v) + dv_{xx} + dv_{yy} \tag{31}$$

where $F(u,v) = f(u,v) + z_1E(u - \bar{u}_0)/L + 2(u - \bar{u}_0)/L^2$ and $G(u,v) = g(u,v) + z_2Ed(v - \bar{v}_0)/L + 2d(v - \bar{v}_0)/L^2$. We thus distinguish between the pairs of modified reaction terms F, G and f, g by the presence and absence of the discretized terms respectively. The modification of the reaction terms through approximation of discrete representation of gradients leaves the structure of the steady state unchanged although the stability of the steady state changes, in general. Two pertinent points are noteworthy. The approximation holds if the thickness of the layer is small and the average of the steady state values of the upper and the lower layers is nearly the same inside the layer; or in other words the perturbation should not be large. Again the layer must be thick enough to allow the formation of spatial structure for a finite residence time of the reaction intermediate and a spatial extension of the order of a wavelength. We now recall the condition for homogeneous steady state u_0, v_0, to be stable if inequalities (12) are satisfied and unstable if

$$f_u + g_u > 0 \tag{32}$$

where f_u, g_u are the derivatives of the functions f and g with respect to u and v, evaluated at the u_0, v_0, respectively. Allowing now perturbation to grow spatially as well as temporarily around u_0, v_0, in the form

$$u(x,y,t) - u_0 \sim e^{\lambda t} \cos k_x x \cos k_y y \tag{33}$$

$$v(x,y,t) - v_0 \sim e^{\lambda t} \cos k_x x \cos k_y y \tag{34}$$

where x, y span the reaction domain defined as $x \in (0, L_x)$ and $y \in (0, L_y)$, we now impose the zero flux boundary conditions as usual, corresponding to eqs. (33) and (34). The linear stability analysis of the eqs. (30) and (31) then leads to the following characteristic equation for λ of the stability matrix

$$\lambda^2 - m\lambda + h = 0 \tag{35}$$

where m and h are given by

$$m(E) = -k^2(1 + d) + F_u + G_u \tag{36}$$

$$h(E) = \left(F_u - k^2\right)\left(G_u - dk^2\right) - F_u G_u \tag{37}$$

and $k^2 = k_x^2 + k_y^2$. Eqs. (36) and (37) include both the effects of diffusion and electric field. The condition for instability within quasi-two dimensional approximation of the reaction diffusion system is given by

$$Re\lambda\left(k^2\right) > 0. \tag{38}$$

To illustrate we now return to chlorite-iodide-malonic acid reaction (CIMA). In presence of electric field along a direction perpendicular to the reaction plane the system of equations become

$$u_t = a - u - 4uv/\left(1+u^2\right) + z_1 E u_z + u_{xx} + u_{yy} + u_{zz} \tag{39}$$

$$v_t = \sigma\left[b\left(u - uv/\left(1+u^2\right)\right)\right] + z_2 \sigma d E v_z + \sigma d\left[u_{xx} + u_{yy} + u_{zz}\right]. \tag{40}$$

To verify the instability condition eq. (38) for pattern formation we resort to numerical simulation in three dimensions. We fix the experimentally admissible parameter values a = 18.0, b = 1.5 d=1.6. In view of a possible experimental arrangement as reported earlier [64], where the electric field strength had been varied over a range between zero to 1 volt/cm, we set our scale of electric field parameter as E = 1 corresponding to 0.2 volt/cm. In our numerical simulation that follows in the subsequent section we have varied E between zero to 0.38 volt/cm. For further analysis we distinguish between the following two situations.

B. Differential flow induced transition of Hopf instability to Turing instability :

We now start with an unstable homogeneous steady state of the system instead of an uniform stable state as in the Turing case. A sufficient condition for this to hold good is eq. (32). Inclusion of the effect of diffusion may, however, bring in stability to this state (in absence of the field) provided the condition $m(0) < 0$, $h(0) > 0$ is satisfied. To achieve this situation we need to satisfy the appropriate boundary conditions. A simple analysis shows that for a fixed set of kinetic parameters and the ratio of the diffusion coefficients that determine $k^2 > k_m^2, k_-^2 > k^2 = \left(n^2\pi^2/L_x^2 + m^2\pi^2/L_y^2\right) > k_+^2$. Here k_m^2 is the zero of $m(0) = 0$ and k_+^2, k_-^2 are the zeros of $h(0) = 0$ when solved for k^2. The unstable wavelengths can therefore be eliminated by fixing the appropriate boundaries of lengths L_x, L_y of the reaction plane, n and m being integers. By switching on the electric field along z direction we then inquire about the stability of the system. It is immediately apparent that a series of wave numbers k^2 that make $m(E) > 0$ and bring in instability lie in the range $0 < k^2 < k_{max}^2$ where k_{max}^2 is a zero of $m(E)=0$ and is given by $k_{max}^2 = \left(1/(1+d)\right)\left[\left(z_1 E/L + z_2 Ed/L\right) + \left(f_u + g_v\right)\right] + 2/L^2$. The positivity of k^2 is ensured for the field E greater than a critical field strength $E_c = -[L(f_u + g_v) + 2(1 + d)] / L(z_1 + z_2 d)$. In order to realize the field-induced instability in the reaction-diffusion system in

quasi-two dimensions we first return to eqs. (39) and (40) and note that the parameter is controlled by the concentration of starch, the Hopf curve, below which one observes the stable oscillation, is given by (note that the diffusion and the electric field terms in Z-direction appear in the effective reaction terms F and G in our analysis)

$$\sigma b = (3a/5) - (25/a) + \left(E/L(z_1 + z_2 d) + 2/L^2(1+d)\right)(5/a + a/5) \tag{41}$$

In Figure 3 we plot Hopf curve shown by the dotted lines for $\sigma = 6$ in absence presence of the field. It is important to note that as the electric field E is increased the Hopf curve shifts downwards. The solid line in Figure 3 is the Turning bifurcation curve in absence of field obtained from the condition $h(0) = 0$ and is given by

$$\left(3da^2 - 5ab - 125d\right)^2 = 100abd\left(25 + a^2\right). \tag{42}$$

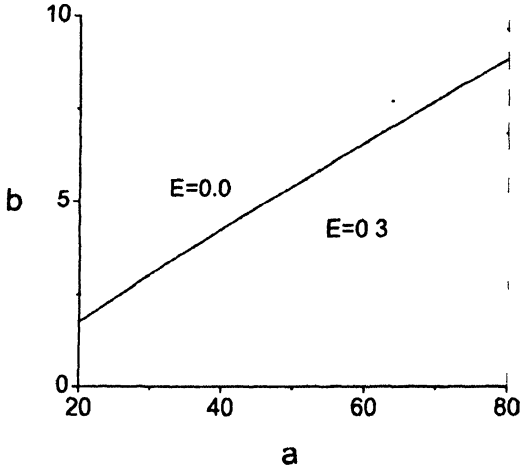

Figure 3. Bifurcation curves : Plot of a *vs* b for the parameter set d=1.6, $\sigma = 4.5$

The homogeneous stable steady state is unstable below this line. We thus observe that as E is increased the Hopf curve falls below the turning line. Since Turing patterns appear below this line we expect that when the electric field is strong enough, it pushes the Hopf curve below the Turing line inducing a transition of Hopf instability to Turing instability and initiates a spatial pattern. For this quasi-two dimensional analysis of formation of field-induced pattern the computations are performed using eqs.(30) and (31) employing the discretization scheme by the explicit Euler method on a 100x100 array in the xy plane with a grid spacing $\Delta x = \Delta y =$ 0.25 and L=10.0 and a time step $\Delta t = 0.0005$ and zero flux boundary conditions on x and y directions. The stability of the numerical results has been checked by using different space and time steps. The simulations are started with spatially random perturbation around the steady state $u_0 = a/5$, $v_0 = 1 + u_0^2$ and for $\sigma = 4.5$. For a field strength $E = 0.5$ we observe in Figure 4(b) a typical stationary spatially pattern in the form of spots, while at $E = 0.0$ the system remains spatially homogeneous. The stationarity of the spatial patterns in all cases is

reached around 10^5 time steps. We note that the transition of instability from Hopf to Turing type inducing pattern formation is triggered only for a critical strength of electric field.

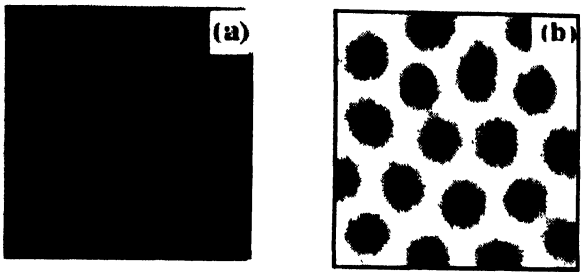

Figure 4 (a,b). Numerically simulated (in two-dimensional space) field induced spatial pattern in CDIMA system.

The above quasi-two-dimensional analysis of stability and the corresponding numerical simulations are, however, not complete in some sense. This is because of the approximation of discretization along z direction and the neglect of variation of concentration along this direction whose importance lies for the electric field to have an effect on the stability of the system. Or in other words it is necessary to go beyond discretization scheme for the electric field term as well as for the diffusion term along z direction and solve eqs. (39) and (40) directly in 3-dimensions. The observation of the differential flow induced transition of Hopf instability can then only be confirmed by such an analysis. With this in mind we have carried out numerical computation with eqs. (39) and (40) using the Euler method for the same set of parameters on a full three-dimensional system. Our detailed analysis indicates that for small thickness of the reaction domain quasi-two dimensional approach is quite satisfactory. However for larger thickness the analysis tends to loose its validity and the system approaches homogeneity.

C. Effect of electric field on Turing instability :

We now explore the effect of constant electric field on Turing instability. We first consider a spatially homogeneous stable steady state corresponding to the condition (8). The necessary and sufficient condition for diffusion-driven Turing instability in absence of any external forcing is $h(0) < 0$. When the electric field is switched on we expect it to modify the instability condition and distort the pattern formation by virtue of the condition $m(E) > 0$.

To investigate the effect of electric field on stationary Turing pattern in CDIMA system, we now restore the Turing space with $\sigma = 8.0$ by adjusting the initial concentration of starch. The conditions eq. (8) and eq.(12) now ensure the Turing condition for diffusion-driven instability in absence of electric field. The computations are performed using eq. (39) and (40) on a three dimensional grid 100x100x10 array in the xy plane with grid spacing $\Delta x = \Delta y = 0.25$ and with $\Delta z = 2$ and a time step $\Delta t = 0.0005$ under zero flux boundary conditions on all sides. In the zero field situation ($E = 0$) one observes the usual Turing pattern in the form of spots as shown

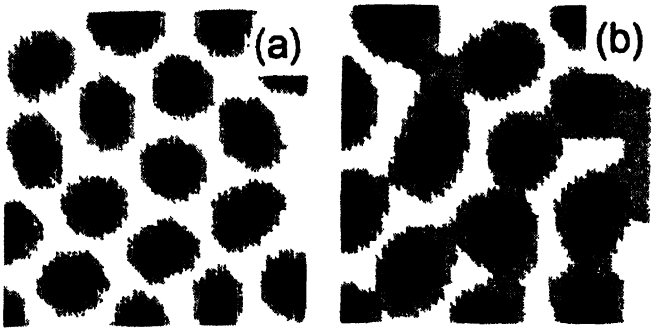

Figure 5(a,b). Numerically simulated (in three dimensional space) field distorted Turning pattern in CIMA system.

of spots as shown in Figure 5(a). When the field strength is increased to $E = 0.4$ spots tend to distort as shown in Figure 5(b). The destabilization of Turing pattern is thus a result of field-modified Turing instability condition.

The above consideration is based on the reaction-diffusion system subjected to a constant electric field normal to the reaction plane. It may be pertinent to ask what happens if the constant electric field lies in the reaction plane. This problem has been addressed recently from an experimental point of view [61]. It has been observed that Turing pattern gets destabilized because of distortion of the structure along the direction of the field. In what follows we revisit this specific issue to bring it in relation to the above theoretical analysis. To this end we must emphasize two points. First, our earlier analysis being based on the application of the field normal to the reaction plane is untenable in such a situation. Second, the spatiotemporal perturbation of the form $\exp(\lambda t)\cos k_x x \cos k_y y$ does not conform to zero flux boundary conditions when the field is applied along, say x-direction of the reaction plane, since the field destroys the nodal structures along this direction. We therefore modify the eqs.(39) and (40) for the present analysis by replacing the terms $z_1 E u_z$ and $z_2 E d\sigma v_z$ by $z_1 E u_x$ and $z_2 E d\sigma v_x$ respectively and discarding the diffusion in z direction and then resort to direct numerical simulation in the Turing parameter space with $\sigma = 8.0$. We carry out the numerical computations on a 100×100 array with grid spacing $\Delta x = \Delta y = 0.25$ and a time step $\Delta t = 0.0005$ and the zero flux boundary conditions. In absence of the field ($E = 0$) one observes the usual Turing spots. When the field strength E along x direction is low (0.4), the spots tend to get distorted along the direction of the field as shown in Figure 6(a) which is close to experimental situation. For a stronger field ($E > 0.5$) deformation of Turing pattern is relatively larger so that the nodes along $x$direction start disappearing Figure 6(b) according to theoretical expectation. We thus observe that depending on its direction a constant electric field may induce an instability in a way that the spatial structure of inhomogeneity differs significantly as illustrated in Figure 5 and Figure 6. Secondly, we emphasize that the formation of spatial pattern in Figure 4, originates from a transition of Hopf instability to Turing instability triggered by the field, vanishes completely when the field is switched off and is therefore generically different from the destabilization of Turing pattern by an application of the constant field.

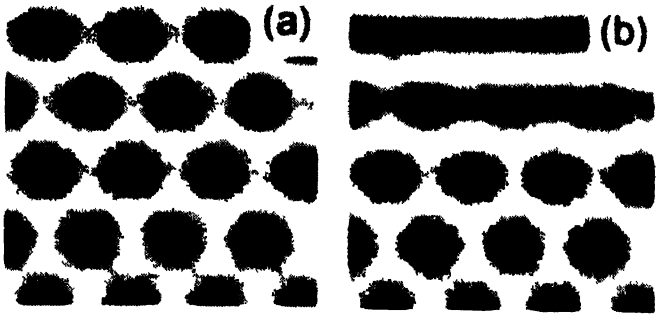

Figure 6 (a,b). Numerically simulated (in two dimensional) field distorted Turing pattern in CIMA system

4. Reaction-Diffusion system in crossed electric and magnetic fields

It is well known that magnetic field can significantly effect a number of chemical reactions which include, for example, geminate radical pair recombination [74–76], auto-oxidation of benzaldehyde by oxygen catalyzed by Co(II) ions [77–79] The conspicuous feature of these work is the paramagnetic nature of the key reacting species. Several living systems are also susceptible to the variation of magnetic field. Can a magnetic field induce pattern due to differential flow in a reaction-diffusion system even when the reacting species are not paramagnetic? We are to show in this section that this differential flow induced pattern may appear for a critical range of magnetic field strength, but this vanishes beyond a spatial extension of the reaction domain normal to the reaction plane [80] We consider a reaction-diffusion system in three dimensions in presence of crossed electric and magnetic fields

$$u_t + \nabla . J_u = f(u,v) \tag{43}$$

$$u_t + \vec{\nabla} . \vec{J_u} = g(u,v) \tag{44}$$

$J_i (i = u,v)$ is the flux of concentration of the i^{th} species $c_i (i = u,v)$ and is comprised of two terms which are due to spatial diffusion and applied field of forces as follows,

$$\vec{J_i} = -D_i \vec{\nabla} c_i - m_i \vec{F_i} c_i \tag{45}$$

D_i is the diffusion coefficient of the i^{th} species and m_i is given $m_i = D_i / kT$, *where k and T* are the Boltzmann constant and temperature, respectively. The Lorentz force experienced by the i^{th} ionic species with velocity v_i and charge $z_i|e|$ due to the electric field $\vec{E}$ and the magnetic field $\vec{B}$ is given by $\vec{F_i} = z_i|e|\left(\vec{E} + \vec{v_i} \times \vec{B}\right)$. The divergence of concentration flux therefore yields

$$\vec{\nabla} . \vec{j} = -D\nabla^2 c_i - z_i|e|(D_i / kT)\vec{\nabla} . \left(\vec{E} + \vec{v_i} \times \vec{B}\right) c_i . \tag{46}$$

To proceed further we first assume that the constant electric field is weak and generates a

steady electric current $\vec{J}$ so that the displacement current term can be neglected from Maxwell's equation to obtain $\vec{\nabla}\times\vec{B}=\mu\vec{J},\mu$ being the permeability of the medium. Since by Ohm's law we have $\vec{J}=\sigma_e\left(\vec{E}+\vec{v}\times\vec{B}\right)$ and $\vec{\nabla}.\vec{\nabla}\times\vec{B}=0$ where σ_e refers to electrical conductivity, one obtains

$$\nabla.\vec{J}=\sigma_e\vec{\nabla}.\left(\vec{E}+\vec{v}\times\vec{B}\right)=0. \tag{47}$$

Therefore from eqs. (45) we are led to the following equation:

$$\vec{\nabla}.\vec{j}_i=-D_i\nabla^2c_i-z_i|e|(D_i/kT)\left(\vec{E}+\vec{v}_i\times\vec{B}\right).\vec{\nabla}c_i. \tag{48}$$

We now consider a reaction with negative ions only. An electric field is applied along *x*-direction to the reaction plane *xy* which has a finite but small extension along *z* direction. This causes a flow or drift current in the negative *x*-direction. In addition a magnetic field *B* lying in the reaction plane points in the positive *y*-direction. As a result the Lorentz force acts to deflect the negative ions in the *z*-direction. Because of accumulation of opposite charges on both sides of the reaction plane, a Hall electric field E^H builds up in the *Z*-direction that balances the Lorentz force in the steady state and current flows only in the *x*-direction. The situation is depicted in Figure 7. Also the spatial extension of the *xy* reaction plane is assumed to

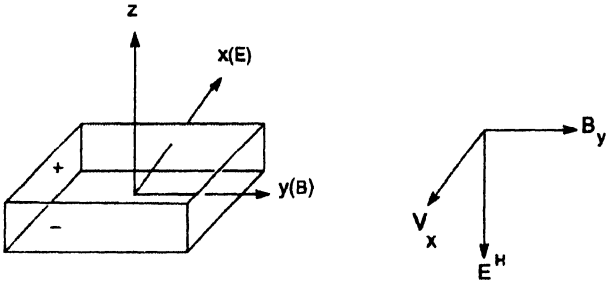

Figure 7. The schematic experimental setup for the reaction-diffusion system in crossed fields.

be much larger compared to that in *z*-direction so that one may comprehend a differential flow along this direction. Thus the layer must be thick enough to allow the formation of spatial structure for a finite residence time of the reaction intermediate and a spatial extension of the order of a wavelength. In accordance with the condition for Hall effect we therefore assume that the velocity $\vec{v}_i$ of the ions is essentially due to the drift [81,82] because of the constant electric field so that by Einstein's relation we may use $\vec{v}_i=z_i|e|(D_i/kT)\vec{E}$.

This implies we neglect altogether any effect to diffusion current. We then arrive at the following two equations.

$$u_t = f(u,v) + D_u\nabla^2 u + z_u|e|(D_u / kT)\vec{E}.\vec{\nabla}u + \left(z_u|e|D_u / kT\right)^2 \vec{E}\times\vec{B}.\vec{\nabla}u \tag{49}$$

$$u_t = g(u,v) + D_u\nabla^2 u + z_u|e|(D_v / kT)\vec{E}.\vec{\nabla}u + \left(z_v|e|D_v / kT\right)^2 \vec{E}\times\vec{B}.\vec{\nabla}v \tag{50}$$

eqs. (49) and (50) form the basis of our analysis that follows.

A. Differential flow induced chemical instability due to crossed fields :

In the presence of crossed fields *i.e.*, electric along x and magnetic field along y direction the system of equations get modified into (taking $z_u = z_v = -1$ and putting U and V for X and Y while emploring eqs. (13) and (14).

$$U_t = k_1' - k_2'U - 3k_3'\frac{UV}{\left(\alpha + U^2\right)} + D_U\nabla^2 U - |e|(D_u / kT)\vec{E}.\vec{\nabla}U + \left(|e|D_u / kT\right)^2 \vec{E}\times\vec{B}.\vec{\nabla}U \tag{51}$$

$$(1/\sigma)V_t = k_2'U - k_3'\frac{UV}{\left(\alpha + U^2\right)} + D_u\nabla^2 V - |e|(D_u / kT)\vec{E}.\vec{\nabla}V + \left(|e|D_u / kT\right)^2 \vec{E}\times\vec{B}.\vec{\nabla}V. \tag{52}$$

Now we substitute $u = \frac{U}{\sqrt{\alpha}}, v = \frac{k_2'V}{k_2'\alpha}, x' = x\left(k_2' / D_u\right)^{1/2}, y' = y\left(k_2' / D_u\right)^{1/2}, z' = z\left(k_2' / D_u\right)^{1/2}$, $t' = k_2't$, to obtain

$$u_t = a - u - 4uv / \left(1 + u^2\right) - \psi u_x + \phi u_z + u_{xx} + u_{yy} + u_{zz} \tag{53}$$

$$(1/\sigma)v_t = \left[b\left(u - uv / \left(1 + u^2\right)\right)\right] - d\psi v_x + d^2\phi v_z + d\left[v_{xx} + v_{yy} + v_{zz}\right]. \tag{54}$$

Here ψ, ϕ, the electric and magnetic field containing terms are abbreviated as $\psi = E\frac{|e|}{kT}(D_u / k_2')^{1/2}$, $\phi = EB\left(\frac{|e|}{kT}\right)^2 D_u\left(k_2' / D_u\right)^{1/2}$. Furthermore we have put $a = \frac{k_1'}{k_2'\sqrt{\alpha}}$, $b = \frac{k_3'}{k_2'\sqrt{\alpha}}$. Also d is the ratio of the diffusion coefficients $(d = D_v / D_u)$ of the activator $\left(ClO_2^-\right)$ and inhinitor $\left(I^-\right)$. All the quantities d, a, b, u, v, x', y', z', t' as well as y and f in eqs. (53) and (54) are dimensionless. (for simplicity, from now onwards we drop the prime (') from x', y', z', t'.

It may be recalled that the homogeneous steady state is unstable below the Turing line. Also as one increase σ, the control parameter, the Hopf line shifts downwards and once it crosses the Turing line diffusion-driven instability sets in resulting in initiation of pattern formation under suitable boundary condition [83]. We now show that the application of crossed electric and magnetic fields, however, may shift the boundary line below the Hopf curve (for the same value for which no instability arises in absence of fields) giving rise to differential flow induced chemical instability and pattern selection.

The crossed field induced instability can be examined by a linear stability analysis of the

system (53,54). To this end we begin with their linearized version as

$$\partial u_t = f_u \partial u + f_v \partial v - \psi \partial u_x + \phi \partial u_z + \partial u_{xx} + \partial u_{yy} + \partial u_{zz} \tag{55}$$

$$\partial v_t = g_u \partial u + g_v \partial v - d\psi \partial v_x + d^2 \phi \partial v_z + d\partial u_{xx} + d\partial v_{yy} + d\partial v_{zz} \tag{56}$$

where $\partial u = u(x, y, z, t) - u_0$ and $\partial v = v(x, y, z, t) - v_0$ are small deviations from homogeneous steady state values u_0 and v_0, respectively. f_u, f_v, g_u, g_v are the partial derivatives of the reaction terms, evaluated at the steady state. A closer look into the linearized equations reveals that a Turing like form of the spatio-temporal perturbation ∂u and ∂v (as $\cos k_x x \cos k_y y \cos k_z z \exp(-\lambda t)$, k_x, k_z and λ being the wave vectors and frequency, respectively) can not work because of the presence of the spatial first derivative terms. However the presence of these terms suggests that they are reminiscent of the differential flow induced terms as discussed in the earlier section. To explore the role of spatially localized perturbation in a similar spirit we take resort to spatial Fourier expansion of the form

$$(\partial u, \partial v) = \frac{1}{2\pi} \int^{\infty} (\quad)$$

Here λ satisfies the following relation which is obtained by making use of the said form of the spatio-temporal perturbation

$$\begin{aligned} &\lambda^2 - \left[f_u - ik_x\psi + ik_z\phi - k_x^2 - k_y^2 + \sigma g_v - i\sigma k_x d\psi + i\sigma k_z d^2\phi - \sigma d k_x^2 - \sigma d k_y^2 - \sigma d k_z^2\right]\lambda \\ &+\left[f_u - ik_x\psi + ik_z\phi - k_x^2 - k_y^2 - k_z^2\right]\left[\sigma g_v - i\sigma k_x d\psi\right. \\ &\left.+ i\sigma k_z d^2\phi - \sigma d k_x^2 - \sigma d k_y^2 - \sigma k_z^2\right] - \sigma g_u f_u = 0. \end{aligned} \tag{58}$$

The above equation gives the dispersion relation $\lambda = \lambda(k_x, k_y, k_z)$. The equation is too cumbersome to arrive at an explicit analytical condition for instability which is given by $Re\lambda > 0$. Further this is subject to boundary conditions for the spatio-temporal perturbations required for the linear stability analysis. A physically allowed choice is zero concentration gradient at the boundaries, such that $\frac{\delta \partial u}{\delta \xi} = 0$ at $\xi = 0$ and $\xi = L_\xi$, where ξ is x, y or z. We impose similar boundary conditions for ∂v. To understand this effect it is instructive to consider only two discrete modes for ∂u as illustration instead of the integral (57) $Ae^{i(k_x x + k_z z)} \cos k_y y + A' e^{i(k'_x x + k'_z z)} \cos k'_y y$. The application of the above-mentioned boundary conditions leads to

$$\frac{\delta \partial u}{\delta z}_{z=0} = iAk_z e^{ik_x x} \cos k_y y + iA' k'_z e^{ik'_x x} \cos k'_y y = 0 \tag{59}$$

$$\frac{\delta \partial u}{\delta z}\Big|_{z=L_z} = iAk_z e^{ik_x x + ik_z L_z} \cos k_y y + iA' k'_z e^{ik'_x x ik'_z L_z} \cos k'_y y = 0. \tag{60}$$

Multiplying eq. (59) by $\exp(ik_z L)$ and on substraction of the resulting equation from eq. (60) we are led to the condition $\tan k_z L_z = \tan k'_z L_z$. This yields the condition $k_z - k'_z = \frac{2n_z\pi}{L_z}$,

$n_z = 1,2,3.....$ Exactly similar condition may be derived for $k_x - k_x' = \frac{2n_x\pi}{L_x}$, $n_z = 1,2,3.....$.

On the other hand for y-direction the application of zero concentration gradient boundary condition leads to $k_y = \frac{n_y\pi}{L_y}$, $n_y = 1, 2, 3....$

Although illustrated for two nodes it is apparent that the above argument can be extended to higher number of modes further to associate discrete numbers corresponding to wave number components and their combinations. Since λ is a function of three variables $\lambda(k_x, k_y, k_z)$ the search for the positivity of may be carried out by varying any two of them (say k_x, k_y) for a fixed value of the other (say k_z) in a surface plot. We draw two sets of such surface plots for two different k_z values in Figures 8 and 9 . For a suitable choice of the order of k_z we may refer to the condition $k_z - k_z' = \frac{2n_z\pi}{L_z}$. For L_z=10 and lowest n_z (n_z=1) a rough estimate for k_z is

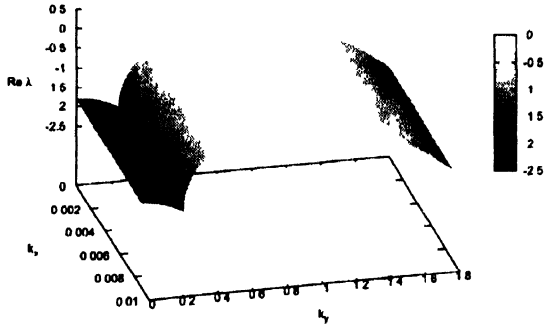

Figure 8. Dispersion relation : Plot of Rel on $k_x - k_y$ plane for $k_z = 0.6$, $\phi = 0.2$.

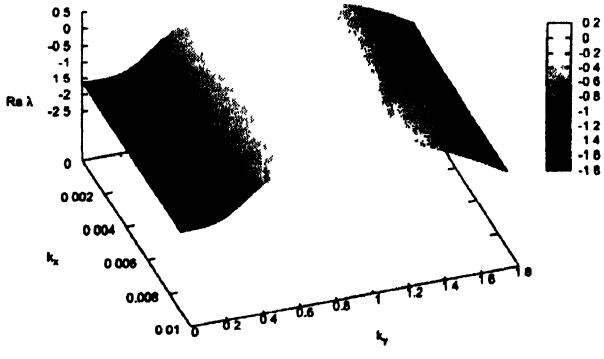

Figure 9. Dispersion relation : Plot of Rel on $k_x - k_y$ plane for $k_z = 0.6$, $\phi = 0.2$.

approximately of the order of 0.6. Keeping in view of this estimate we then fix k_z in Figures 8 and 9 as $k_z = 0.6$ and 1.2 respectively. A closer look into eq. (58) also reveals that as k_x and k_z appear either quadratically or in imaginary part, the dispersion curves remain same for the reversal of sign of *kx* and *kz*. This may also be checked by numerical computation. Thus the positive wave number regions have been plotted in Figures 8 and 9.

In Figures 8 and 9 we draw surface plots for the planes $Re\lambda$ as a function of k_x and k_y for a fixed $k_z = 0.6$, for the parameter set $a = 18.0$, $b = 1.5$, $d = 1.6$, $\sigma = 5.9$ and for a fixed electric field of strength $\Psi = 0.01$ applied along x direction and varied magnetic field strength. All the eigenvalues are negative in absence of magnetic field (ϕ=0.0). The system however for the same parameter set loses stability beyond $\phi = 0.2$.

B. Pattern formation in crossed fields :

Before going over to full numerical simulations it is necessary to introduce the appropriate boundary conditions for the problem described by eq. (53) and eq. (54) involving the differential flow terms due to electric and magnetic fields. In defining the fluxes we take care of the field containing terms as well. Therefore we write for the *u*-component

$$J_x = \frac{\partial u}{\partial x} - \psi u$$

$$J_y = \frac{\partial u}{\partial y}$$

$$J_z = \frac{\partial u}{\partial z} + \phi u \tag{61}$$

and for the *v* component

$$J_x = d\frac{\partial v}{\partial x} - \psi v$$

$$J_y = d\frac{\partial v}{\partial y}$$

$$J_z = d\frac{\partial v}{\partial z} - \phi v .$$

The computations were performed using eqs. (53) and (54) on a three dimensional grid 200 × 200 × 10 with $\Delta x = \Delta y = 1.0$, $\Delta z = 1.0$ and time step $\Delta t = 0.0005$ and with zero flux (concen-

(a) (b) (c)

Figure 10. Numerically simulated magnetic field induced spatial pattern.

tration) boundary conditions. The parameter set used allows the system to stay in the Hopf region for $\sigma = 5.9$ and the system remains homogeneous. The simulations were started with spatially random perturbation of 1% around the steady state. As the constant external electric field (dimensionless value $\psi = 0.01$) is applied along positive x-direction one observes (Figure10) an inhomogeneous spatial structure in the form of stationary spots only when a magnetic field over a certain strength along positive y-direction is applied simultaneously in the reaction plane. Our numerical simulation shows that for the given value of electric field strength the spatial inhomogeneity appears only beyond a critical magnetic field strength (dimensionless value higher than $\sigma = 0.2$). A typical magnetic field induced pattern is drawn in Figure10(b) for $\phi = 0.2$. A comparison between linear stability analysis and numerical simulation in terms of the observed wave numbers seems pertinent. It appears from Figure 9 that instability should appear at k_y close to zero. A look into Figure10 clearly reveals that a distinct wave number can be associated with the numerically simulated pattern. As pointed out earlier the application of zero concentration gradient boundary condition on the spatiotemporal perturbation in the linear stability analysis yields $k_y^2 = n_y^2\pi^2 / L_y^2$. For around ten nodes in the y direction (Figure 11), ($n_y = 10$ and $L_y = 200$, k_y is approximately 0.15 which corroborates with the linear stability analysis. An enlarged version of the selected area of Figure 10(b) is shown in Figure 11. The stable structure tends to vanish at higher strengths of the magnetic field as

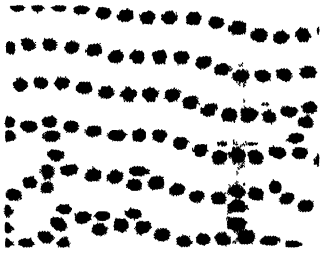

Figure 11. An enlarged picture of a small area (50x50) taken from the net 200 x 299 area shown in Figure 10(b).

shown in Figure 10(c). Our numerical experience shows that beyond a certain thickness of the reaction plane the system tends to be homogeneous. It is therefore apparent that although the activator and the inhibitor ions are diamagnetic in character, the magnetic field in reaction-diffusion system in addition to the diffusional flux along the direction of charge separation plays an important role in pattern formation and selection. We emphasize that the shift of the stability boundary in generating spatial structure due to differential flow by application of magnetic field is different from the scenario that leads to Turing pattern. To illustrate we now consider the following situation. For $\sigma = 7.0$ the reaction-diffusion system in absence of the applied fields exhibits the usual Turing pattern in the form of spots as shown in Figure12(a). Application of the electric and the magnetic fields ($\psi = 0.01$ and $\phi = 0.2$) results in deformation of pattern (Figure 12(b)). As the electric field strength is kept constant and the magnetic field is increased

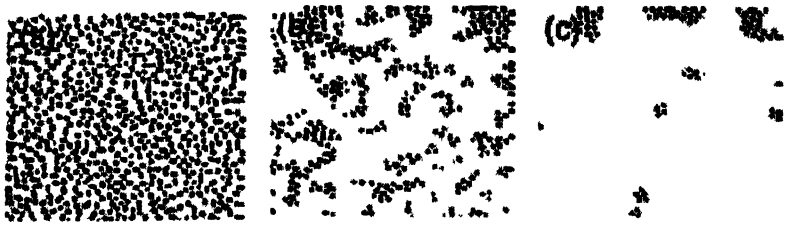

Figure 12. Numerically simulated (in two-dimensions) field distored Turning pattern in CDIMA system.

one observes greater distortion of pattern (Figure 12(c)). Thus the scenarios depicted in Figure 10 illustrating the pattern formation due to differential flow induced instability and those in Figure 12 displaying the modification of Turing pattern by crossed fields are generically distinct.

Before closing this section a few points regarding the observability of the effect in chlorine dioxide-iodide-malonic acid system seems pertinent. To meet the condition of the cross-field effect the reaction plane should be thin but at the same time must allow a perceptible separation of the charges along z direction. Since the effect of electric field on Turing Pattern in this system has already been an aspect of experimental study it is worthwhile to look for the effect by simultaneously applying the magnetic field with implementation of such a set-up. The required magnitude of the electric and magnetic field strength E and B may be estimated in actual terms from the dimensionless expressions $\psi = \frac{E|e|}{kT}\left(\frac{D_u}{k_2}\right)^{1/2} = \frac{EF}{RT}(D_u / k_2')^{1/2}$ and $\phi = EB\left(\frac{|e|}{kT}\right)^2 D_u(k_2' / D_u)^{1/2} = EB\left(\frac{F}{RT}\right)^2 D_u(D_u / k_2')^{-1/2}$ where k_2' is expressed as k_2 times initial concentration of ClO_2, $[ClO_2]0$. Putting $k_2 = 6x10^3 mole^{-1}, [ClO_2]_0 = (1/6)x10^{-3}$ moles/lit and $D_{ClO_2}(=D_u) = 1\times10^{-5} cm^2$ / sec one requires the electric field E as 0.06 volt/cm to correspond $\psi = 0.01$ and magnetic field B as 60 Gauss to correspond $\phi = 0.1$ at temperature 25^0C to realize a typical pattern induced by crossed-fields.

5. Conclusion

The spontaneous formation of structure in spatially extended systems under far from equilibrium condition is an active area of wide current interest. In this review we have given a pedagogical exposition of Turing pattern and its experimental realization in a reaction diffusion system which describes an interplay of kinetics of activator and inhibitor and diffusive motion. Turing pattern is a result of local activation and long range inhibition.The reaction-diffusion system specialized for ionic reactions has been further subjected to electric and/or magnetic fields to explore another kind of instability. This differential flow induced instability is a consequence of convective terms with differential mobility of the two species. We have shown specifically in the context that a constant electric field when applied normal to the quasi-two dimensional reaction plane may induce a transition of Hopf instability to Turing instability due to this differential convective flow. The scenario is distinctly different from deformed Turing pattern in presence of

an electric field. This differential flow and the associated instability can also be achieved when the reaction-diffusion system is placed in crossed electric and magnetic fields lying on the reaction plane. The resulting pattern formation is again generically different from Turing pattern and the instability conditions are irrespective of the ratio of diffusivities being unity.

As pointed out earlier the discovery of CDIMA system opened up new possibilities in the field. This not only includes the development of other pattern forming systems but also involves the role of various external factors inducing instability, studying the phenomena beyond two dimensions, effect of coupling between two systems *etc.* The field also ramified to finding out biological systems and the respective morphogens responsible for pattern formation.

Very recently interest has been shown on pattern formation in systems beyond two dimensions. Reaction-diffusion systems *viz.* the Brusselator and the Gray-Scott model in three dimensions are numerically studied to obtain several interconnected structures of domains as well as lamellar, hexagonal and spherical domains as stable motionless equilibrium patterns [25]. Turing pattern on a sphere was considered earlier by Bhattacharya [26] with the help of Galerkin model. A reaction-diffusion system with conserved mass has been investigated recently [27]. The patterns generated need not be stationary in all cases. Oscillatory Turing patterns in the form of spots (often called the 'twinkling eyes'), localized spiral or concentric within spot-like or stripe-like Turing structure have been reported when coupling between two adjacent Turing layers were considered [29]. Later another study with this coupled system revealed that changing the coupling strength causes an interesting transition from a superposition of Turing structure and a super lattice pattern [30]. The effect of parametric modulation on pattern formation has also been studied [86].

Another extension of the theory is its application to developmental biology. Many plausible models based on reaction coupled with diffusion have been proposed for bones, skin organs, butterfly wing patterns, animal coat markings. In these models hypothetical chemicals called the morphogens react and diffuse and as a consequence of which under certain conditions a homogeneous steady state evolves into a heterogeneous one. The cells may be able to interpret the local concentrations of the morphogens and differentiate accordingly giving rise to patterned structure. This is the concept of "positional information" as proposed by Wolpert [87]. The reaction diffusion model by Thomas based on empirical chemical laws is able to reproduce patterns observed in animal coat markings. Pattern formation thus promises to remain an active area for some more years to come.

Acknowledgement

We thank S. Kar, S. Banarjee, S. Dutta and S. Sen for valuable discussions over the years and their active cooperation.

References

[1] A T Fechner *Schweigg J.* **53** 61 (1828)

[2] W C Bray *J. Am.* Chem. Soc. **43** 1262 (1921)

[3] W C Bray *J. Am.* Chem. Soc. **53** 38 (1931)

[4] W Ostwald *Phys. Zeitsch.* **8** 87 (1899)

[5] B P Belousov *Sbornik Referatov po Radiatsionni Meditsine* **145** (1981)

[6] B P Belousov *Oscillations and travelling waves in Chemical Systems* R J Field, M Burger (Eds.) (New York : Wiley) 605 (1985)

[7] P De Keeper J Boissonade and IR Epstein, *J. Phys. Chem.* **94** 6525 (1990)

[8] V Castets, E Dulos, J Boissonade and P De Keeper *Phys. Rev. Lett.* **64** 2953 (1990)

[9] V Castets, E Dulos and J Boissonade *Physica* **49D** 2161 (1991)

[10] Q Quang and H L Swinney *Nature* **352** 610 (1991)

[11] I Lengyel and I R Epstein Proc. *Natl. Acad. Sci* **89** 3977 (1992)

[12] S S Riaz, S Kar and D S Ray *J. Chem. Phys.***121** 5395 (2004)

[13] S S Riaz, S Kar and D S Ray *Physica* D **203** 224 (2005)

[14] I Lengyel and I R Epstein *Science* **251** 650 (1991)

[15] M Menzinger and A B Rovinsky *In Chemical Waves and Patterns* edited by R Kapral and K Showalter (Kluwer, Dordrecht) 365 (1992)

[16] A M Turing *Philos. Trans. R Soc London* **327** 37 (1952)

[17] I R Epstein and J A Pojman *An Introduction to Nonlinear Chemical Dynamics* (Oxford University Press) (1998)

[18] W Y Tam, W Horsthemke, Z Noszticzius H L Swinney and *J Chem Phys.* **88** 3395(1988a)

[19] R A Bario, C Varea, J Aragon and P K Maini *Bull. Math. Biol.* **61** 483 (1999)

[20] E E Selkov *Eur J Biochem.* **4** 79 (1968)

[21] A Goldbeter and R Lefever *Biophys. J.* **12** 1302 (1972)

[22] S Kar and D S Ray *Phys. Rev. Lett.* **90** 238102 (2003)

[23] A Goldbeter *Biochemical Oscillations and Cellular Rhythms. The Molecular Bases of Periodic and Chaotic behaviour* (Cambridge : Cambridge University Press) (1996)

[24] For a detailed discussion see J D Murray *Mathematical Biology* (Springer) (1989)

[25] H Shoji, K Yamada, D Ueyama and T Ohta *Phys. Rev.* **E 75** 046212 (2007)

[26] S Bhattacharya *Phys. Rev.* **E 72** 036208 (2005)

[27] S Ishihara, M Otsuji and A Mochizuki *Phys. Rev.* E **75** 015203 (2007)

[28] T Schwartz, T Carmon, H Buljan and M Segev *Phys. Rev. Lett.* **93** 223901 (2004)

[29] L Yang I Epstein *Phys. Rev. Lett.* **90** 178303 (2003)

[30] I Berenstein, M Dolnik, L Yang, A M Zhabotinisky and I Epstein *Phys. Rev.* **E 70** 046219 (2004)

[31] H C Tuckwell and R M Miura *Biophysical Journal* **23** 257 (1978)

[32] F Siegert and C Wejer *J. Cell. Sci.* **93** 325 (1993)

[33] S Jakubith, H H Rotermund, W Engel, A Von Oertzen and G Ertl *Phys. Rev. Lett.* **65** 3013 (1990)

[34] P Chamacho and J D Lechleiter *Science* **260** 226 (1993)

[35] J M Davidenko, A V Pertsov, R Salomonsz, W Baxter and J Jalife *Nature* **355** 349 (1992)

[36] T Plesser, S C Müller and B Hess *J. Phys. Chem.* **94** 7501 (1990)

[37] A T Winfree and W Jahnke *J. Phys. Chem.* **93** 2823 (1989)

[38] *Chemical Waves and Patterns* edited by R Kapral and K Showalter (Kluwer, Derducht) (1993)

[39] M C Cross and P C Hohenberg *Rev. Mod. Phys.* **65** 851(1993)

[40] J P Keener and J J Tyson *Physica* **D21** 307(1986)

[41] D S Cohen, J C Neu and R R Rosales *SIAM J. Appl. Math.* **35** 536 (1978)

[42] M R Duffy, N F Britton and J D Murray *SIAM J. Appl. Math.* **39** 8 (1980)

[43] N Kopell and L N Howard *Adv. Appl. Math.* **2** 417(1981)

[44] A S Mikhailov and V I Krinsky *Physica* D9 346 (1983)

[45] F H Busse *J. Math. Phys.* **46** 140(1967); F H Busse *Rep. Prog. Phys.* **41** 1929 (1978)

[46] A C Newell and J A Whitehead *J Fluid Mech* **38** 279(1969)

[47] V Eckhaus *'Study in Nonlinear Stability Theory'*, Springer Tracts in Natural Philosophy, **Vol.6** (Berlin : Springer-Verlag)

[48] L Kramer, H R Schober and W Zimmermann *Physica* **D 31** 212 (1988)

[49] M Lowe and J P Gollub *Phys. Rev. Lett.* **55** 2575 (1985)

[50] Carl M Bender and Steven A Orszag *Advanced Mathematical Methods For Scientists and Engineers* (McGrow-Hill Book Company)

[51] K J Painter, P K Maini and H G Othmer, *Proc. Natl. Acad. Sci. U. S. A.* **96** 5549 (1999)

[52] A Gierer and H Meinhardt *Kybernetik* **12** 30 (1982)

[53] H Meinhardt *Models of Biological Pattern Formation* (London : Academic) (1982)

[54] J D Murray *Mathamatical Biology* (Berlin : Springer-Verlag) (1993).

[55] A B Rovinsky and M Menzinger *Phys. Rev.* Lett. **69** 1193 (1992)

[56] A B Rovinsky and M Menzinger *Phys. Rev.* Lett. **70** 778 (1993)

[57] S S Riaz, S Kar and D S Ray *J. Chem. Phys.***121** 5395 (2004)

[58] O Jensen, V O Pannbacker, E Mosekilde G Dewel and P Borckmans *Phys. Rev.* **E 50** 736 (1994)

[59] S Haris *J. Phys.* **A 36** 8291 (2003)

[60] J Yang, F Xie, Z Qu and A Garfinkel *Phys. Rev. Lett.* **91** 1483021 (2003)

[61] B Schmidt, P DeKepper and S C Müller *Phys. Rev. Lett.* **90** 118302 (2003)

[62] I Berenstein, L Yang, M Dolnik, A M Zhabotinsky and I R Epstein *Phys. Rev. Lett.* **91** 058302 (2003)

[63] A K Horvath, M Dolnik, A P Munuzuri, A M Zhabotinsky and I R Epstein *Phys. Rev. Lett.* **83** 2950 (1999)

[64] B Schmidt, P DeKepper and S C Müller *Phys. Rev. Lett.* **90** 118302 (2003)

[65] H Sevelkova and M *Marek Physica* **D 9** 140 (1983)

[66] H Sevelkova and M *Marek Physica* **D 21** 61(1986)

[67] A F Münster, P Hasal, D Snita and M Marek *Phys. Rev.* **E 50** 546 (1994)

[68] S Schimdt and P Ortoleva *J. Chem. Phys.* **74** 4488 (1981)

[69] H Sevelkova, M Marek and S C Müller *Science* **257**; *Phys. Rev. Lett.* **69** 2729 (1992)

[70] A De Wit *Adv. Chem. Phys.* **109** 435(1999)

[71] A De Wit, D Lima, G Dewel and P Borckmans *Phys. Rev* **E54** 261 (1996)

[72] G Dewel, A De Wit, S Metens, Berdasca and P Borckmans *Physica Scripta* T67 **51** (1996)

[73] B Rudovics, E Dulos and P De Kepper *Physica Scripta* T67 **43** (1996)

[74] E Steiner and T Ulrich *Chem. Rev.* **89** 51 (1989)

[75] K Bhattacharyya and M Chowdhury *Chem. Rev.* **93** 507 (1993)

[76] M Halder, P P Parui, K R Gopidas, D N Nath and M Chowdhury *J. Phys. Chem.* **A 106** 2200 (2002)

[77] E Boga, Kadar, G Peintler and I Nagypal *Nature* **347** 749 (1990)
[78] X He, K Kustin, I Nagypal and G Peintler *Inorg. Chem.* **33** 2077(1994)
[79] J D Lechleiter and D E Clapham *Cell* **69** 283 (1992)
[80] S S Riaz, S Banarjee, S Kar and D S Ray *Eur. Phys. J.* **B 53** 509 (2006)
[81] H Sevcikova and M Marek *Physica D* **9** 140 (1983)
[82] H Sevcikova and M Marek *Physica D* **21** 61 (1986)
[83] O Jensen, V O Pannbacker, E Mosekilde, G Dewel and P Borckmans *Phys. Rev. E* **50** 736 (1994)
[84] A F Munster, F Hasal, D Smita and M Marek *Phys. Rev. E* **50** 546 (1994)
[85] A B Rovinsky and M Menzinger *Phys. Rev. Letts.* **69** 1193 (1992)
[86] A Bhattacharyay and J K Bhattarjee *Eur. Phys. J.* B21 561 (2001)
[87] L Wolpert *J Theor. Biol.* **25** 1(1969)